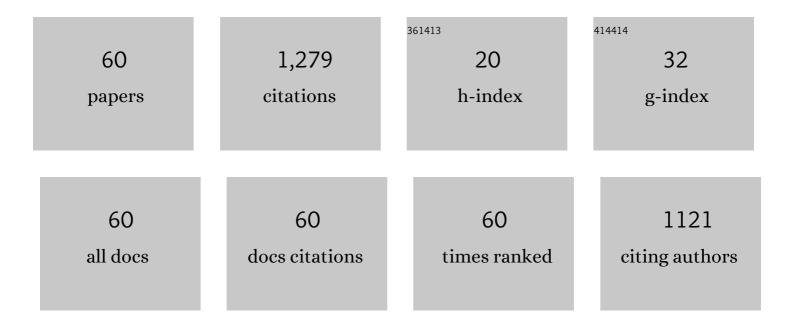
Stephan Orzada

List of Publications by Year in descending order

Source: https://exaly.com/author-pdf/2291112/publications.pdf Version: 2024-02-01



#	Article	IF	CITATIONS
1	Multi-echo fMRI of the cortical laminae in humans at 7T. NeuroImage, 2011, 56, 1276-1285.	4.2	152
2	RF excitation using time interleaved acquisition of modes (TIAMO) to address <i>B</i> ₁ inhomogeneity in highâ€field MRI. Magnetic Resonance in Medicine, 2010, 64, 327-333.	3.0	115
3	An Eight-Channel Phased Array RF Coil for Spine MR Imaging at 7 T. Investigative Radiology, 2009, 44, 734-740.	6.2	71
4	A 32-channel parallel transmit system add-on for 7T MRI. PLoS ONE, 2019, 14, e0222452.	2.5	48
5	Evaluation of Hardware-related Geometrical Distortion in Structural MRI at 7 Tesla for Image-guided Applications in Neurosurgery. Academic Radiology, 2011, 18, 910-916.	2.5	37
6	Dynamic Contrast-Enhanced Renal MRI at 7 Tesla. Investigative Radiology, 2011, 46, 425-433.	6.2	37
7	Feasibility of <i>T</i> ₂ -weighted turbo spin echo imaging of the human prostate at 7 tesla. Magnetic Resonance in Medicine, 2014, 71, 1711-1719.	3.0	36
8	In vivo ³¹ P MR spectroscopic imaging of the human prostate at 7 T: Safety and feasibility. Magnetic Resonance in Medicine, 2012, 68, 1683-1695.	3.0	34
9	MR safety assessment of potential RF heating from cranial fixation plates at 7 T. Medical Physics, 2013, 40, 042302.	3.0	33
10	Image quality and cancer visibility of T2-weighted Magnetic Resonance Imaging of the prostate at 7 Tesla. European Radiology, 2014, 24, 1950-1958.	4.5	32
11	7T ultraâ€high field body <scp>MR</scp> imaging with an 8â€channel transmit/32â€channel receive radiofrequency coil array. Medical Physics, 2018, 45, 2978-2990.	3.0	32
12	Timeâ€interleaved acquisition of modes: An analysis of SAR and image contrast implications. Magnetic Resonance in Medicine, 2012, 67, 1033-1041.	3.0	30
13	Bilateral hip imaging at 7 Tesla using a multi-channel transmit technology: initial results presenting anatomical detail in healthy volunteers and pathological changes in patients with avascular necrosis of the femoral head. Skeletal Radiology, 2013, 42, 1555-1563.	2.0	28
14	Renal imaging at 7 Tesla: preliminary results. European Radiology, 2011, 21, 841-849.	4.5	27
15	³¹ P MR spectroscopic imaging of the human prostate at 7 T: T ₁ relaxation times, Nuclear Overhauser Effect, and spectral characterization. Magnetic Resonance in Medicine, 2015, 73, 909-920.	3.0	27
16	Impact of different meander sizes on the RF transmit performance and coupling of microstrip line elements at 7 T. Medical Physics, 2015, 42, 4542-4552.	3.0	27
17	Fast and accurate multiâ€channel mapping based on the TIAMO technique for 7T UHF body MRI. Magnetic Resonance in Medicine, 2018, 79, 2652-2664.	3.0	26
18	Contrast-enhanced ultra-high-field liver MRI: A feasibility trial. European Journal of Radiology, 2013, 82, 760-767.	2.6	22

STEPHAN ORZADA

#	Article	IF	CITATIONS
19	Cardiac MRI: evaluation of phonocardiogram-gated cine imaging for the assessment of global und regional left ventricular function in clinical routine. European Radiology, 2012, 22, 559-568.	4.5	21
20	First-pass contrast-enhanced renal MRA at 7ÂTesla: initial results. European Radiology, 2013, 23, 1059-1066.	4.5	21
21	Parallel transmit capability of various RF transmit elements and arrays at 7T MRI. Magnetic Resonance in Medicine, 2018, 79, 1116-1126.	3.0	21
22	Magnetic Resonance Imaging of Cranial Nerves at 7ÂTesla. Clinical Neuroradiology, 2013, 23, 17-23.	1.9	20
23	Phosphorus Magnetic Resonance Spectroscopic Imaging at 7 T in Patients With Prostate Cancer. Investigative Radiology, 2014, 49, 363-372.	6.2	20
24	Optimized 31 P MRS in the human brain at 7 T with a dedicated RF coil setup. NMR in Biomedicine, 2015, 28, 1570-1578.	2.8	20
25	Hip imaging of avascular necrosis at 7 Tesla compared with 3 Tesla. Skeletal Radiology, 2014, 43, 623-632.	2.0	19
26	An 8/15â€channel Tx/Rx head neck RF coil combination with regionâ€specific B ₁ + shimming for wholeâ€brain MRI focused on the cerebellum at 7T. Magnetic Resonance in Medicine, 2018, 80, 1252-1265.	3.0	19
27	USPIO-enhanced MRI of pelvic lymph nodes at 7-T: preliminary experience. European Radiology, 2019, 29, 6529-6538.	4.5	17
28	Impact of repetitive exposure to strong static magnetic fields on pregnancy and embryonic development of mice. Journal of Magnetic Resonance Imaging, 2014, 39, 691-699.	3.4	16
29	1 H MR spectroscopic imaging of the prostate at 7 T using spectralâ€spatial pulses. Magnetic Resonance in Medicine, 2016, 75, 933-945.	3.0	16
30	High resolution <scp>MR</scp> imaging of pelvic lymph nodes at 7 Tesla. Magnetic Resonance in Medicine, 2017, 78, 1020-1028.	3.0	16
31	Analysis of an Integrated 8-Channel Tx/Rx Body Array for Use as a Body Coil in 7-Tesla MRI. Frontiers in Physics, 2017, 5, .	2.1	16
32	Open design eightâ€channel transmit/receive coil for highâ€resolution and realâ€time ankle imaging at 7 T. Medical Physics, 2011, 38, 1162-1167.	3.0	15
33	Mitigation of <i>B</i> ₁ ⁺ inhomogeneity on singleâ€channel transmit systems with TIAMO. Magnetic Resonance in Medicine, 2013, 70, 290-294.	3.0	14
34	Performance analysis of integrated RF microstrip transmit antenna arrays with high channel count for body imaging at 7 T. NMR in Biomedicine, 2021, 34, e4515.	2.8	14
35	Sequence Comparison for Non-Enhanced MRA of the Lower Extremity Arteries at 7 Tesla. PLoS ONE, 2014, 9, e86274.	2.5	14
36	Initial Evaluation of Non–Contrast-Enhanced Magnetic Resonance Angiography in Patients With Peripheral Arterial Occlusive Disease at 7 T. Investigative Radiology, 2014, 49, 331-338.	6.2	13

STEPHAN ORZADA

#	Article	IF	CITATIONS
37	Seven-Tesla MRI of the female pelvis. European Radiology, 2013, 23, 2364-2373.	4.5	12
38	Development and evaluation of a 16â€channel receiveâ€only RF coil to improve 7T ultraâ€high field body MRI with focus on the spine. Magnetic Resonance in Medicine, 2019, 82, 796-810.	3.0	12
39	Nonenhanced Magnetic Resonance Angiography of the Lower Extremity Vessels at 7 Tesla. Investigative Radiology, 2013, 48, 525-534.	6.2	9
40	T1-Weighted Contrast-Enhanced Magnetic Resonance Imaging of the Small Bowel. Investigative Radiology, 2015, 50, 539-547.	6.2	9
41	An 8â€channel transceiver 7â€channel receive <scp>RF</scp> coil setup for high <scp>SNR</scp> ultrahighâ€field <scp>MRI</scp> of the shoulder at 7T. Medical Physics, 2017, 44, 6195-6208.	3.0	9
42	Performance and safety assessment of an integrated transmit array for body imaging at 7ÅT under consideration of specific absorption rate, tissue temperature, and thermal dose. NMR in Biomedicine, 2022, 35, e4656.	2.8	9
43	Design and comparison of two eightâ€channel transmit/receive radiofrequency arrays for <i>in vivo</i> rodent imaging on a 7 T human wholeâ€body MRI system. Medical Physics, 2010, 37, 2225-2232.	3.0	8
44	Repetitive exposure of mice to strong static magnetic fields in utero does not impair fertility in adulthood but may affect placental weight of offspring. Journal of Magnetic Resonance Imaging, 2014, 39, 683-690.	3.4	8
45	Non-enhanced magnetic resonance imaging of the small bowel at 7 Tesla in comparison to 1.5 Tesla: First steps towards clinical application. Magnetic Resonance Imaging, 2016, 34, 668-673.	1.8	8
46	A method to approximate maximum local SAR in multichannel transmit MR systems without transmit phase information. Magnetic Resonance in Medicine, 2017, 78, 805-811.	3.0	8
47	Local SAR compression with overestimation control to reduce maximum relative SAR overestimation and improve multi-channel RF array performance. Magnetic Resonance Materials in Physics, Biology, and Medicine, 2021, 34, 153-163.	2.0	8
48	Local SAR compression algorithm with improved compression, speed, and flexibility. Magnetic Resonance in Medicine, 2021, 86, 561-568.	3.0	8
49	Ultrahigh-Field Imaging of the Biliary Tract at 7 T. Investigative Radiology, 2014, 49, 346-353.	6.2	7
50	Contrast enhanced renal MR angiography at 7 Tesla: How much gadolinium do we need?. European Journal of Radiology, 2017, 86, 76-82.	2.6	7
51	A multitransmit external body array combined with a ¹ H and ³¹ P endorectal coil to enable a multiparametric and multimetabolic MRI examination of the prostate at 7T. Medical Physics, 2019, 46, 3893-3905.	3.0	6
52	Magnetic resonance imaging at ultra-high magnetic field strength: An in vivo assessment of number, size and distribution of pelvic lymph nodes. PLoS ONE, 2020, 15, e0236884.	2.5	5
53	Cardiac magnetic resonance: is phonocardiogram gating reliable in velocity-encoded phase contrast imaging?. European Radiology, 2012, 22, 2679-2687.	4.5	4
54	Comparison of Fat Saturation Techniques for Single-Shot Fast Spin Echo Sequences for 7-T Body Imaging. Investigative Radiology, 2014, 49, 101-108.	6.2	4

#	Article	IF	CITATIONS
55	Parasitic element based decoupling of 7 tesla MRI coil array. , 2015, , .		4
56	Postâ€processing algorithms for specific absorption rate compression. Magnetic Resonance in Medicine, 2021, 86, 2853-2861.	3.0	4
57	Feasibility of aortic valve planimetry at 7 T ultrahigh field MRI: Comparison to aortic valve MRI at 3 T and 1.5 T. European Journal of Radiology Open, 2018, 5, 159-164.	1.6	2
58	Investigation of the Saturation Pulse Artifact in Non-Enhanced MR Angiography of the Lower Extremity Arteries at 7 Tesla. PLoS ONE, 2015, 10, e0119845.	2.5	2
59	A Fast Technique to Calculate the First Physical Modes of Conductors over a Wide Frequency Range. , 2005, , .		0
60	In vivo MRI of the human torso at 7 Tesla using multi-channel transmit. , 2010, , .		0